INTERNATIONAL JOURNAL FOR NUMERICAL METHODS IN FLUIDS
Int. J. Numer. Meth. Fluids 2008; **56**:1255–1260
Published online 17 December 2007 in Wiley InterScience (www.interscience.wiley.com). DOI: 10.1002/fld.1649

Mesh movement *via* Legendre transforms

R. D. Giddings[1,*,†] and M. J. P. Cullen[2]

[1]*AWE, Aldermaston RG7 4PR, U.K.*
[2]*Met Office, Fitzroy Road, Exeter EX1 3PB, U.K.*

SUMMARY

A new mesh movement algorithm is presented based on a Legendre transform arising from optimal transportation theory. This naturally allows the mesh connectivity to change, so that adjacent cells can move apart to avoid regions of distorted or poor quality mesh. It is applied here to the Euler equations with conservation on such a mesh achieved by the construction of space–time cells. The method is demonstrated on problems with large deformations and where the regions of concentrated mesh change their topology, e.g. merging and separating. © British Crown Copyright 2007/MOD. Reproduced with permission. Published by John Wiley & Sons, Ltd.

Received 13 May 2007; Revised 12 July 2007; Accepted 25 September 2007

KEY WORDS: mesh movement; optimal transportation; monitor functions

1. INTRODUCTION

A large class of current algorithms for governing mesh motion (e.g. [1–3]) are based on *harmonic maps*, which minimize the elastic energy stored in the deformation of the current mesh from a reference mesh. Monitor functions are used to specify the coefficients of elasticity at each point in the mesh, so that it concentrates where desired.

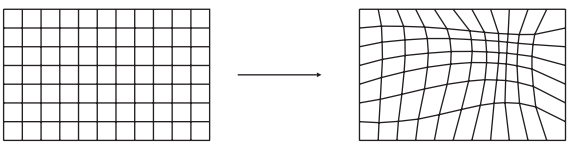

*Correspondence to: R. D. Giddings, AWE, Aldermaston RG7 4PR, U.K.
†E-mail: r.d.giddings@reading.ac.uk

This model requires the deformation to be differentiable with the result that the mesh connectivity must remain fixed which can result in areas of distorted or poor quality cells.

Optimal transportation theory [4] considers a closely related problem, where again one region must be deformed into another but now any movement incurs a given cost, for example, being proportional to the distance moved. Specifically, an initial distribution μ of some quantity, e.g. sand in a heap, is to be transported into a final distribution v of the same total volume.

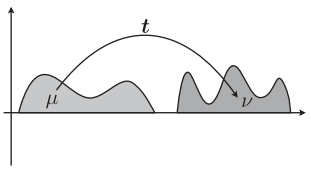

The adapted mesh is generated by minimizing the total transportation cost $I[\mathbf{t}]=\int c(\mathbf{x},\mathbf{t}(\mathbf{x}))\,\mathrm{d}\mu(\mathbf{x})$, where $c(\mathbf{x},\mathbf{y})$ is the cost of moving a unit of sand from $\mathbf{x}$ to $\mathbf{y}=\mathbf{t}(\mathbf{x})$. It is no longer important to the total cost whether initially adjacent points remain close or not, which means that neighbouring cells in the reference mesh can end up being moved apart in the deformed mesh, although in practice they do not move far. As with harmonic maps, existence and uniqueness of minimizers (for convex regions and cost functions) has been proved but numerical solution techniques are still evolving. Here one such method—the *geometric method* [5], originating from meteorology [6]—is applied to the Euler equations.

2. MESH CONSTRUCTION USING THE LEGENDRE TRANSFORM

The key result is that for quadratic cost ($c(\mathbf{x},\mathbf{y})=|\mathbf{x}-\mathbf{y}|^2$), the optimal transport plan, when it exists, is of the form $\mathbf{t}=\nabla\varphi(\mathbf{x})$ for some convex scalar function φ. Furthermore, $\mathbf{x}=\nabla_{\mathbf{t}}\psi(\mathbf{t})$ where ψ, φ are *Legendre–Fenchel* transforms of each other—an extension of the more familiar Legendre transform to functions that are not convex or differentiable.

The general strategy of the geometric method is to iteratively improve φ until $\mathbf{t}=\nabla\varphi(\mathbf{x})$ correctly transports μ into v. The Legendre–Fenchel transform of a convex piecewise linear function is another convex piecewise linear function, hence provides simple approximations for φ and ψ that can exactly satisfy the transform criterion. The projections of φ, ψ onto their base planes then constitute the reference and deformed meshes. We set $\mu=1$ and v to be concentrated on a fixed set of points, one for each cell, the mass of each then setting a target area for that cell. The vertices of ψ are located at the fixed set, and on iteration the heights are adjusted by the conjugate gradient method to minimize the difference between the actual and target areas. This raises or lowers the faces of φ with gradient unchanged, which can result in changes to the connectivity of the mesh, e.g. as shown below, where cells a and c move apart and cells b and d become new neighbours:

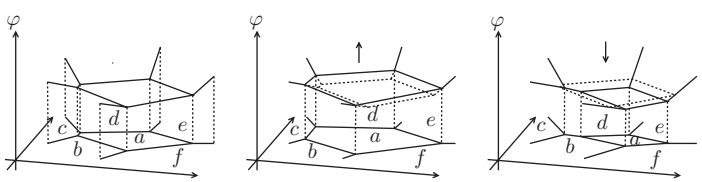

DOI: 10.1002/fld

For efficiency, instead of constructing a new mesh from scratch each iteration [5], the *panel beater* algorithm [6, Section 5.3.2, 7] modifies the current mesh, locally adjusting the connectivity as required. Cells could be added or removed with a similar procedure. The geometric method extends naturally to higher dimensions and has been implemented in three dimensions, but the explicit geometric repair in the panel beater algorithm becomes increasingly complex.

3. APPLICATION TO THE EULER EQUATIONS

A 2D second-order Godunov (MUSCL-Hancock) scheme, adapted from Azarenok *et al*. [8], is applied to the standard Euler equations for a perfect fluid with reflective or transmissive boundary conditions. In it time is used as the third dimension and the mesh at the start of the time step is 'joined up' to the mesh at the end to create space–time cells.

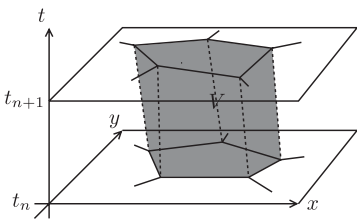

When a connectivity change occurs this leaves a tetrahedral 'gap' that is split into four sub-tetrahedra each assigned to it's neighbouring cell.

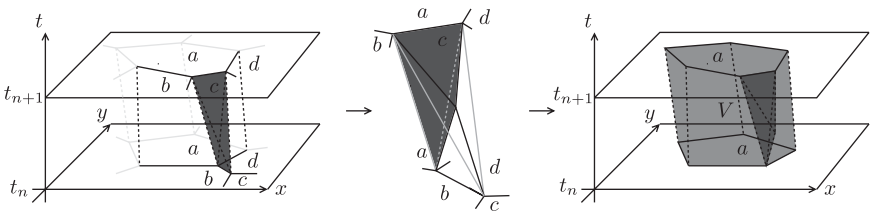

The flow variables at t_{n+1} are used to determine the monitor functions and hence set new cell areas at t_{n+1} according to the equidistribution criterion, $a_i m_i = \text{constant}$, for area a_i and scalar monitor m_i in cell i. A mesh intensity parameter α is also used [3]. The mesh at t_{n+1} is adjusted by the geometric method to realize these new cell areas and the flow variables re-evaluated. These steps are iterated a fixed number of times or until the mesh movement drops below a tolerance or adjacent connectivity changes occur (which happens occasionally in practice).

4. MONITOR FUNCTION

The mesh movement scheme is global—on changing the area of a single cell the entire mesh moves to accommodate it. For the above iteration to converge, the monitor needs to have minimal

DOI: 10.1002/fld

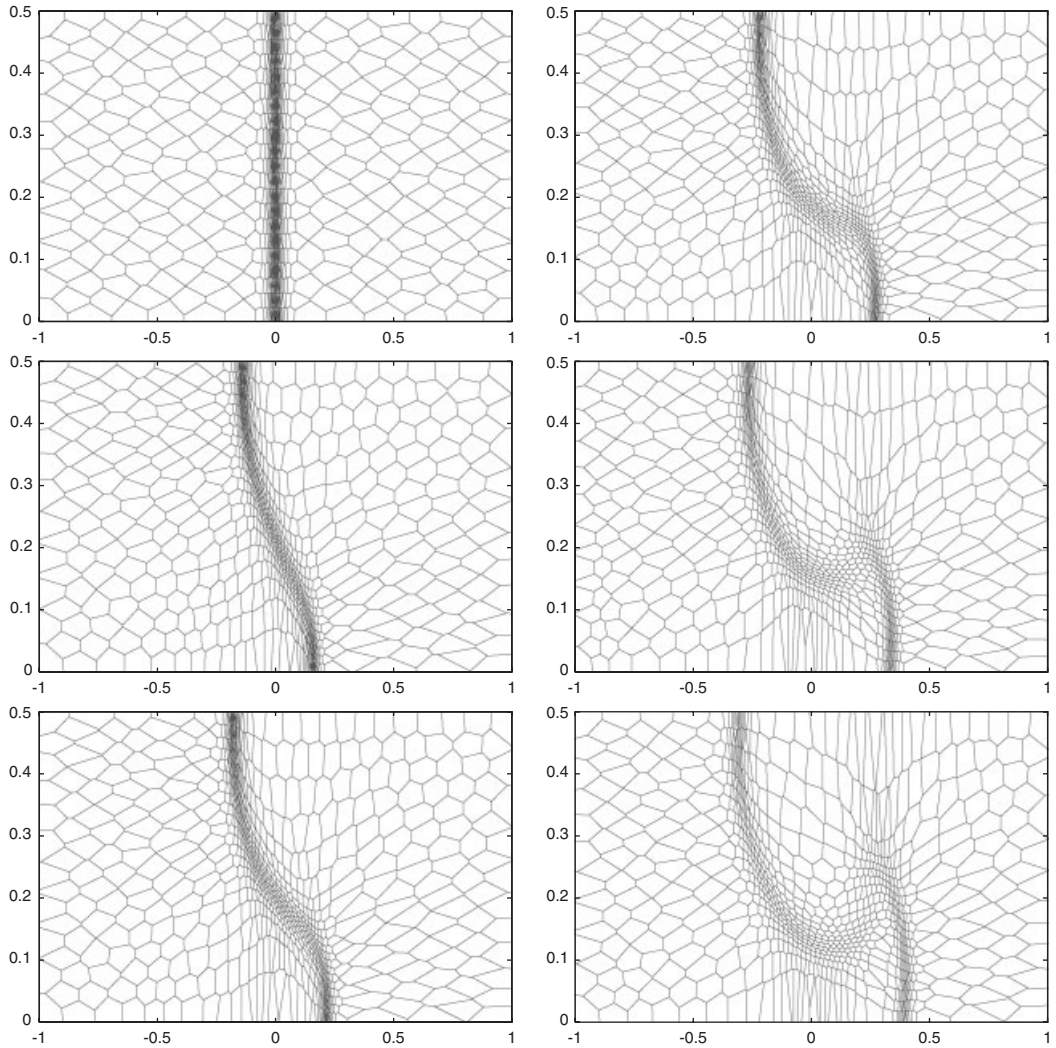

Figure 1. Rayliegh–Taylor instability ($t=0$, 0.172, 0.248; 0.341, 0.471, 0.626; 855 cells).

mesh dependence in the presence of discontinuities in the flow variables from, e.g. shocks. To this end, the moving least-squares method [9] is employed. The error in a variable f is $E_i(\mathbf{x})=\int_{|\mathbf{x}'-\mathbf{x}|\leqslant h} w(|\mathbf{x}'-\mathbf{x}|)[f(\mathbf{x}')-\bar{f}_i(\mathbf{x}')]^2\,\mathrm{d}\mathbf{x}'\approx\sum_j w_j[f_j-\bar{f}_i(\mathbf{x}'_j)]^2$, where f_j is the cell average of f in cell j, $w_j=a_j w(r_j)/\sum_k a_k w(r_k)$, where $a_j, \mathbf{x}'_j$ are the area and centroid of the part of cell j inside the circle radius h about $\mathbf{x}$, $r_j=|\mathbf{x}'_j-\mathbf{x}|$ and the weight $w(r)=\cos^2(\pi r/2h)$ here. The approximants $\bar{f}_i(\mathbf{x})$, $i=0,1,2,\ldots$, are constant, linear, quadratic, etc. polynomials in x, y with coefficients determined by minimizing E_i. Here, f is density and instead of, say, the extracted gradient of $\bar{f}_i$, the least-squares errors E_i were found to be the smoothest available quantities. For smooth data, E_0-E_1 is proportional to the gradient (squared) and E_1-E_2 is related to the

DOI: 10.1002/fld

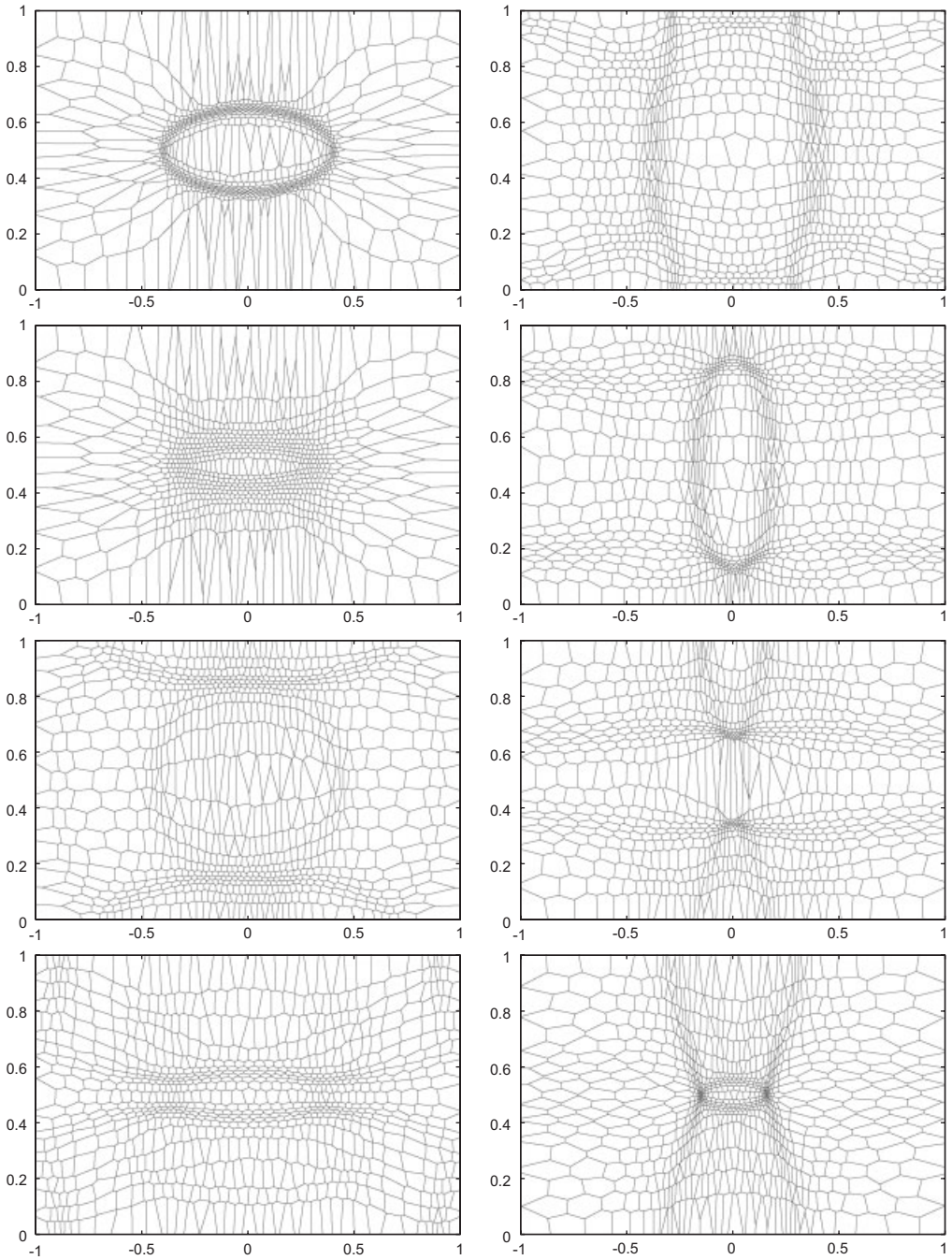

Figure 2. Outward elliptical shock ($t=0$, 0.103, 0.345, 0.624; 1.121, 1.293, 1.441, 1.602; 855 cells).

DOI: 10.1002/fld

principal curvatures. For nonsmooth data, these errors are still smooth, being proportional to the jump in monitor (squared). For the Sod shock tube at $t=0.6$ s, these errors are (density in red, E_0, E_1, E_2 (scaled) are green, pink and blue).

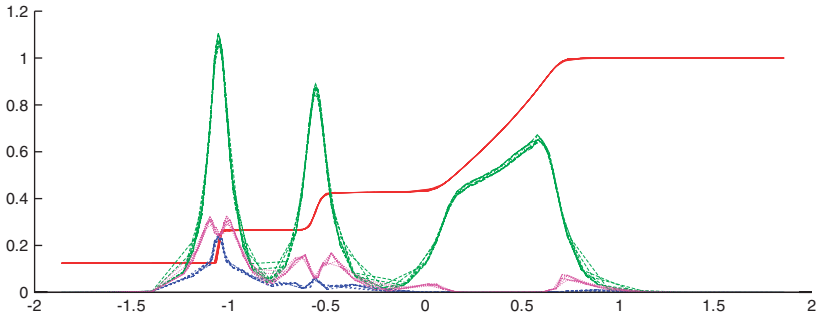

Theoretically $E_1, E_2, \ldots$ can be used to distinguish discontinuities from smoother regions in the flow, but as seen above they are slightly noisier and bias towards shocks more than E_0.

5. RESULTS

(1) *Rayleigh–Taylor instability*: The initial conditions are: $\rho=2.0$ (lhs), 1.0 (rhs), $g=1.0$ (to the right), $u=ke^{-2\pi x}\cos(2\pi y)$, $v=ke^{-2\pi x}\sin(2\pi y)$, where $k=1.02$ and the pressure so as to be in equilibrium. For this problem, the monitor $m=E_1+E_2$ is successful (Figure 1).

(2) *Elliptical shock*: Initially $\rho=p=1$ inside the ellipse $(x/0.4)^2+(y/0.3)^2=1$, $\rho=0.125$, $p=0.1$ outside. Figure 2 shows the mesh adapting as the regions requiring more mesh move around the domain and change topology, although few cells are used to properly resolve discontinuities. The previous monitor proved unsatisfactory; hence, here $m=E_0+0.1E_1+0.01E_2$.

The problems ran in 62 and 43 min, respectively, on a PC (AMD Athlon 3800 CPU).

REFERENCES

1. Winslow A. Numerical solution of the quasi-linear Poisson equation in a nonuniform triangular mesh. *Journal of Computational Physics* 1967; **1**:149.
2. Brackbill JU. An adaptive grid with directional control. *Journal of Computational Physics* 1993; **108**:38–50.
3. Huang W. Practical aspects of formulation and solution of moving mesh partial differential equations. *Journal of Computational Physics* 2001; **171**:753–775.
4. Villani C. Topics in optimal transportation. *Graduate Studies in Mathematics*, vol. 58. American Mathematical Society: Providence, RI, 2003.
5. Chynoweth S. The semi-geostrophic equation and the Legendre transform. *Ph.D. Thesis*, University of Reading, 1987.
6. Cullen MJP. *A Mathematical Theory of Large-scale Atmosphere/Ocean Flow*. Imperial College Press: London, 2006.
7. Purser RJ. Private communication, 1991.
8. Azarenok BN, Ivanenko SA, Tang T. Adaptive mesh redistribution method based on Godunov's scheme. *Communications in Mathematical Sciences* 2003; **1**(1):153–180.
9. Li S, Liu WK. Meshfree and particle methods and their applications. *Applied Mechanics Reviews* 2002; **55**(1): 1–34.

DOI: 10.1002/fld